NANO LETTERS

LETTER

pubs.acs.org/NanoLett

The Influence of Surface Oxide on the Growth of Metal/Semiconductor Nanowires

Kuo-Chang Lu,[*,†,∥] Wen-Wei Wu,[*,‡,∥] Hao Ouyang,[§] Yung-Chen Lin,[⊥] Yu Huang,[⊥] Chun-Wen Wang,[‡] Zheng-Wei Wu,[†] Chun-Wei Huang,[‡] Lih J. Chen,[*,§] and K. N. Tu[⊥]

[†]Department of Materials Science and Engineering, National Cheng Kung University, Tainan 701, Taiwan

[‡]Department of Materials Science and Engineering, National Chiao Tung University, Hsinchu 300, Taiwan

[§]Department of Materials Science and Engineering, National Tsing Hua University, Hsinchu 300, Taiwan

[⊥]Department of Materials Science and Engineering, University of California, Los Angeles, Los Angeles, California 90095-1595, United States

Supporting Information

ABSTRACT: We report the critical effects of oxide on the growth of nanostructures through silicide formation. Under an in situ ultrahigh vacuum transmission electron microscope, it is observed from the conversion of Si nanowires into the metallic PtSi grains epitaxially through controlled reactions between lithographically defined Pt pads and Si nanowires. With oxide, instead of contact area, single crystal PtSi grains start forming either near the center between two adjacent pads or from the ends of Si nanowires, resulting in the heterostructure formation of Si/PtSi/Si. Without oxide, transformation from Si into PtSi begins at the contact area between them, resulting in the heterostructure formation of PtSi/Si/PtSi. The nanowire heterostructures have an atomically sharp interface with epitaxial relationships of Si(20-2)//PtSi(10-1) and Si[111]//PtSi[111]. Additionally, it has been observed that the existence of oxide significantly affects not only the growth position but also the growth behavior and the growth rate by two orders of magnitude. Molecular dynamics simulations have been performed to support our experimental results and the proposed growth mechanisms. In addition to fundamental science, the significance of the study matters for future processing techniques in nanotechnology and related applications as well.

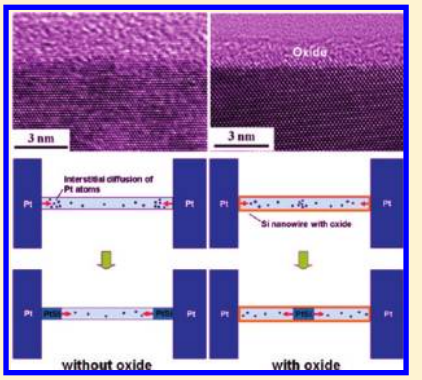

KEYWORDS: Surface oxide, silicide nanowires, nanokinetics, nanoheterostructures, in situ TEM, molecular dynamics simulations

Semiconductor nanowires (NWs) are attractive components for future nanoelectronics since they can exhibit a range of device functions and may serve as active elements in larger scale integration.[1−5] Particularly, nanoscale transistors based on silicon nanowires have been extensively studied[6,7] for their potentials of replacing conventional planar metal-oxide-semiconductor field-effect transistors (MOSFET) in integrated circuits[3,8] and of opening new opportunities in flexible macroelectronics[9−11] and highly sensitive biosensors.[12,13] Oxide is a very common and important material, being indispensible especially in the semiconductor field and Si-based related processing. Additionally here, for Si nanowires, one of the nanostructures having the greatest potential in the future, oxide was even found to be able to affect subsequent processing significantly. Metal silicides are essential as electrical contacts in our current processing of integrated circuits.[14−20] Lithographically defined metal contacts are most often used in silicon nanowire transistors to facilitate the device performance. However, the formation of metal silicide nanowires and the structure and properties of silicide/silicon heterostructures have emerged as interesting problems.[18,19]

According to our experiences on nanoheterostructures,[18,19,21] we believe the surface oxide surrounding Si nanowires is worth studying carefully for being an important factor in silicide formation at nanoscale. Platinum is an interesting interconnecting material for nanoelectronics, being chemically stable in ambient or oxidizing environment. Additionally, metallic platinum silicide (PtSi) can be used as ohmic contact to p-channel Si nanowire transistors.[22] Shown in our previous studies,[21] based on PtSi/Si/PtSi nanowire heterostructures, p-channel enhancement mode nanowire FETs with the best performance from intrinsic Si nanowires have been fabricated. Therefore, we have designed the following experiments, using controlled reactions between lithographically defined Pt pads and Si nanowires with or without oxide under in situ transmission electron microscopy (TEM) for further investigation of the oxide effect on formation of single crystal PtSi and PtSi/Si nanowire heterostructures. In-situ TEM is powerful for the study on growth dynamics.[23−34]

Silicon nanowires were prepared on a p-type Si wafer by the vapor−liquid−solid (VLS) method using nano Au dots as nucleation sites. The resultant single crystal Si

Received: March 28, 2011
Revised: May 22, 2011
Published: June 09, 2011

nanowires are along a [111] growth direction[35−37] and with thin surface oxide (∼1−5 nm thick). The Si nanowires with lengths of a few micrometers ranged in diameter from 10 to 40 nm.

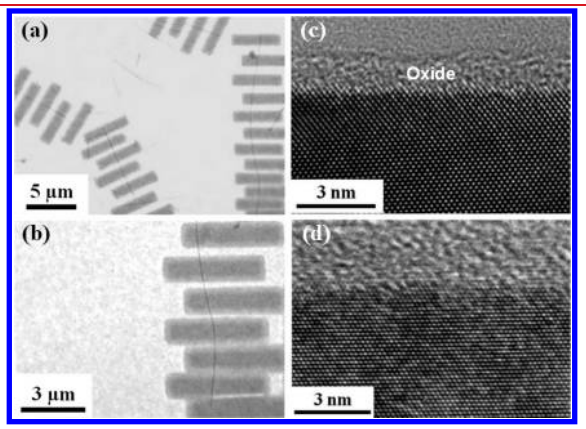

Figure 1. Overview of sample preparation. (a) A TEM image of a sample with multiple sets of a Si nanowire across Pt contact pads. (b) A TEM image showing a closer look at one of the Si NW-Pt pad sets. (c) A HRTEM image of a Si nanowire with 2 nm oxide and with smooth Si/oxide interfaces. (d) A HRTEM image of a Si nanowire without oxide and with rough Si/oxide interfaces.

The Si nanowire samples with Pt contact pads were fabricated on Si/Si_3N_4 substrate using e-beam lithography and e-beam evaporation (Figure 1a and b). Since each of our samples contains multiple Si nanowires and there are many Pt pads deposited on a single nanowire as shown in Figure 1a and b, we can observe numerous examples in one sample and have done so in different samples. All of our observation supports the mechanism we report here. Prior to Pt deposition, some of the Si nanowire samples were etched in buffered hydrofluoric acid for 5 s to remove native oxide at the contact region, while some were not. The etched samples were HF dipped again prior to being loaded in ultrahigh vacuum TEM (UHV-TEM) to prevent native oxide at regions other than contact areas. Figure 1c and d is high-resolution TEM (HRTEM) images showing the samples with and without oxide, respectively; thereby, we can investigate the effect of native oxide on kinetics of phase transformation. For nanowires with HF dipping, no oxide was seen, and the Si/oxide interface was rough. For nanowires without HF dipping, the surface oxide is of 1−2 nm, and the Si/oxide interface was smooth. TEM examinations were conducted in a JEOL 2000 V UHV-TEM under a base pressure of 3×10^{-10} Torr, where

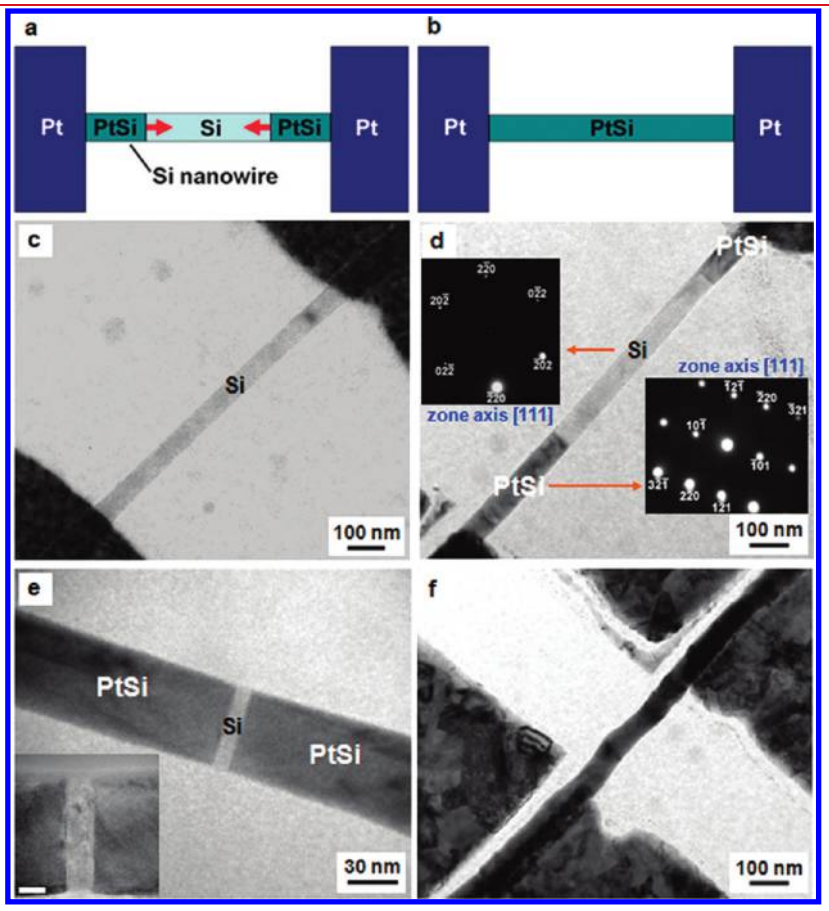

Figure 2. Formation of single crystal PtSi nanowire and PtSi/Si/PtSi nanoheterostructures with varying length of the Si region. (a) A schematic illustration depicting growth of a PtSi/Si/PtSi nanoheterostructure. (b) A schematic illustration showing full transformation from a Si nanowire to a PtSi nanowire. (c) In situ TEM image of a Si nanowire before reaction. (d and e) In situ TEM images showing PtSi/Si/PtSi nanoheterostructures in which the Si regions are 575 and 8 nm in length, respectively. The darker region is PtSi, while the brighter region is Si. The insets in (d) are the corresponding selected area diffraction patterns of Si and PtSi, respectively. The inset in (e) is the magnification of the gap region and the scale bar is 5 nm. (f) In situ TEM image of a PtSi nanowire after reaction and full transformation from Si into PtSi.

dx.doi.org/10.1021/nl201037m |*Nano Lett.* 2011, 11, 2753–2758

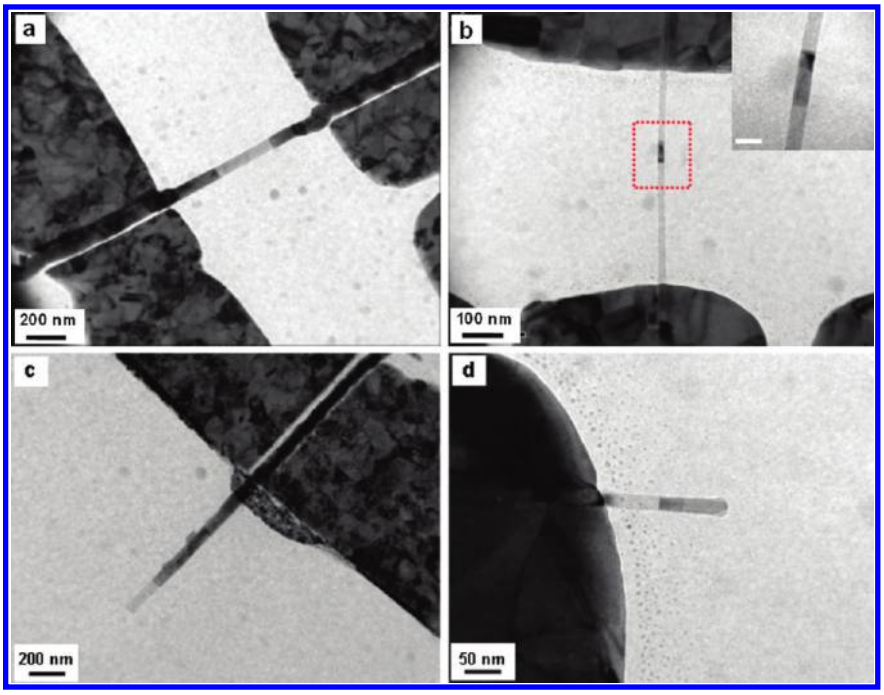

Figure 3. In situ TEM images showing different heterostructures of PtSi/Si based on different growth mechanisms due to oxide effect. (a) In situ TEM image of a PtSi/Si/PtSi heterostructure within a Si nanowire without surface oxide. The bright area is Si, and the dark area is PtSi. (b) In situ TEM image of a Si/PtSi/Si heterostructure within a Si nanowire with surface oxide. The bright area is Si, and the dark area is PtSi. The inset in (b) is magnification of the heterostructure in which the scale bar is 20 nm. (c) In situ TEM image showing the formation of PtSi within an overhang Si nanowire without oxide from a single Pt pad. The PtSi grows from the contact toward the end of the Si. (d) In situ TEM image showing the formation of PtSi within an overhang Si nanowire with surface oxide. The PtSi grows from the end of the Si nanowire toward the Pt pad.

sample can be heated to 1000 °C. Upon heating in UHV-TEM, Pt reacts with Si nanowires to form PtSi nanowires. Phase identification was carried out by electron diffraction pattern and energy dispersion X-ray spectrometer (EDS) analysis.

Electron beam lithography and e-beam evaporation were then used to define and deposit the Pt pads on Si nanowires (Figure 2a). We recall that prior to Pt deposition, some of the samples were etched in buffered hydrofluoric acid for 5 s to remove native oxide. After Pt deposition, the samples are loaded into TEM and annealed in situ at 500 °C to form PtSi (Figure 2b).

Figure 2c shows an etched Si nanowire with Pt pads on both sides before reaction. After annealing at 500 °C for about 5−10 min, higher contrast sections with sharp interface with the Si start to emerge from both ends of the nanowire near the Pt pads, suggesting the formation of PtSi (Figure 2d). This is attributed to the fact that many Pt atoms are able to dissolute into silicon through the long contact between the Si nanowire and the Pt pad so that supersaturation can be reached; thereby, nucleation and growth of PtSi occur below the contact. Utilizing this phenomenon, nanowire heterostructure of PtSi/Si/PtSi, in which the length of the middle Si, can be precisely controlled down to sub-10 nanometer regime (Figure 2e). Upon further annealing, all the Si are consumed and transformed into a PtSi nanowire (Figure 2f). Detachment of wires from pads is due to strain resulting from volume expansion.[21] However, it occurs at a late stage of silicidation, while our point is at the beginning of silicidation; thus, it does not affect the behavior we observed and report. Also, if it had been the stress or contact condition that matters, then we should have observed incoherent behaviors among the many examples of a sample. Additionally, we have previously found that the stress effect is on the phase instead of nucleation sites.[38]

Based on the electron diffraction pattern corresponding to the platinum silicide region (right part of Figure 2d), the silicide material is identified to be single crystal PtSi with an orthorhombic crystal structure having lattice constants a = 0.5567, b = 0.3587, and c = 0.5927 nm. In addition, the epitaxial relationships between Si and PtSi have been determined as Si(20-2)//PtSi(10-1) and Si[111]//PtSi[111], according to the diffraction patterns in Figure 2d.

The effect of surface oxide on PtSi formation is shown in Figure 3. In the TEM images of Figure 3a and c, Si nanowires were HF dipped so that they were free of oxide. At 500 °C, PtSi forms within the Si nanowire from the contact area between the Pt pad and the Si nanowire. However in Figure 3b and d, where Si nanowires were not etched with HF and they had surface oxide of 1−5 nm in thickness, PtSi forms within the Si nanowire near the center of the Si nanowire (Figure 3b) and from the end of the Si nanowire (Figure 3d), respectively. Since all of the phase transformations occurred in the Si nanowires, platinum atoms were the dominating diffusion species. We note that in Figure 3a and b, the Si nanowire was across two Pt contact pads, yet in Figure 3c and d, the Si nanowire was an overhang from one Pt pad.

The different mechanisms in forming different PtSi/Si nanoheterostructures are depicted in Figure 4. Figure 4a and c is the corresponding schematic illustrations of PtSi formation in Figure 3a and c. In terms of nucleation where the PtSi starts, supersaturation of Pt is needed. In Figure 4a, due to no impedance of oxide and due to the line contact between a Pt pad and a Si nanowire, a large number of Pt atoms can quickly dissolve into the Si nanowire. Supersaturation of Pt in the Si nanowire can be

dx.doi.org/10.1021/nl201037m |*Nano Lett.* 2011, 11, 2753–2758

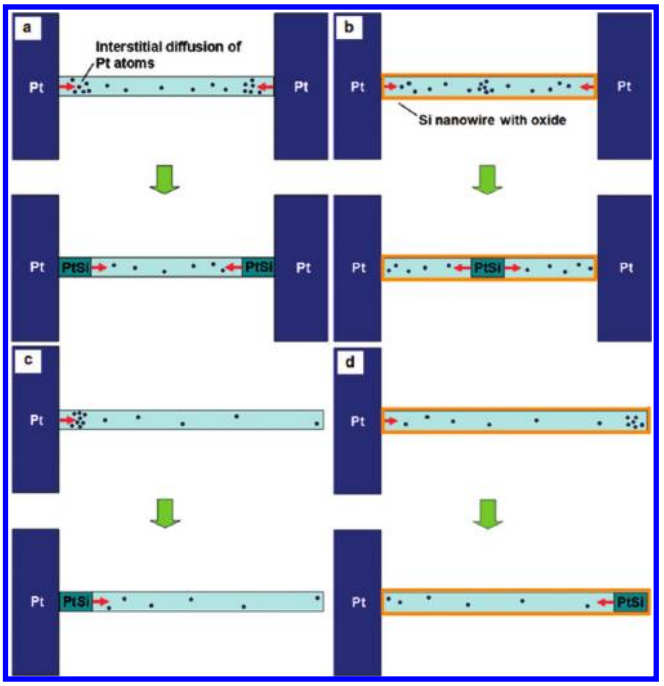

Figure 4. Schematic illustrations of oxide effect on kinetics of nanosilicide formation. (a) A schematic illustration corresponding to Figure 3a, showing growth of a PtSi/Si/PtSi heterostructure within a Si nanowire without oxide. (b) A schematic illustration corresponding to Figure 3b, showing growth of a Si/PtSi/Si heterostructure within a Si nanowire with surface oxide. (c) A schematic illustration corresponding to Figure 3c, showing the PtSi formation within an overhang Si nanowire without oxide. The growth occurs from the Pt pad to an end of the Si nanowire. (d) A schematic illustration corresponding to Figure 3d, showing PtSi formation within an overhang Si nanowire with surface oxide. The growth occurs from an end of the Si nanowire to the Pt pad.

reached below the line contact because of the very low equilibrium solubility of interstitial Pt atoms in Si. Therefore, the nucleation and growth of PtSi starts from the contacts, leading to a PtSi/Si/PtSi heterostructure. Based on the same reason, in Figure 4c, PtSi forms from the contact area between the Pt pad and the overhanging Si nanowire.

Figure 4b and d are the corresponding schematic illustrations of PtSi formations in Figure 3b and d, where the Si nanowire has surface oxide. There are two reasons why nucleation cannot occur at the contact area between the Pt pad and the oxidized Si nanowire. The first is that the oxide on the Si nanowire surface limits the dissolution of Pt atoms into the Si. The second is the very rapid interstitial diffusion of Pt in Si. Thus, whenever a Pt atom has dissolved into the Si nanowire, it will quickly diffuse away, resulting in no supersaturation below the contact and also a very low concentration gradient of Pt atoms over the entire Si nanowire. However, around the center of the Si nanowire in Figure 4b, an accumulation of Pt atoms appears with fluxes of Pt atoms coming from both sides. It is the place where the solubility of interstitial Pt in Si can reach supersaturation first, in turn the nucleation of PtSi, contributing to the formation of a Si/PtSi/Si heterostructure. This is analogous to the chemical reaction between Ni nanodots and a Si nanowire,[39] where NiSi forms between the two Ni nanodots instead of the contact point between the dot and the wire. As for the case of Figure 4d, when Pt atoms diffuse interstitially to the end of the Si nanowire, they will pile up at the end since the reverse diffusion is against the concentration gradient. Again, the PtSi formation in Figure 4d starts at the end of the Si nanowire rather than at the contact.

In our previous reports on point contact reaction between Ni and Si nanowires,[18,19] besides interstitial diffusion of Ni in Si, surface diffusion of Ni on the oxidized Si surface could have been a competing mechanism. Similarly, some might think the Pt−Si reaction here results from surface diffusion. However, surface diffusion fails to explain the silicide formation from the pad−wire contact, as shown here. Also, it cannot explain the silicide formation starting from one end of Si nanowire to Pt pad nor starting near the center between two adjacent pads. On the contrary, interstitial diffusion in a Si nanowire applies to all these conditions very well. Furthermore, we have conducted experiments to demonstrate that these reactions are by interstitial diffusion rather than by surface diffusion.[39] We successfully fabricated multiple silicide/Si nanowire heterostructures through the reaction between Si nanowires and metal nanodots. If it had been surface diffusion, then we should have observed nonstop growth, and the structure could not have been formed; also, we should have observed ripening among the metal nanodots during annealing, but we did not.[39] Therefore, we propose that the reaction in this work is assisted by Pt interstitial diffusion within Si nanowires, since the silicide can be highly deficient in Pt, and there are a large number of vacancies in the sublattice of Pt of the silicide, making the diffusion of Pt through the silicide very fast.

In addition to the impact on the nucleation sites, the existence of oxide affects the rate of silicide formation significantly according to the Supporting Information movies S1 and S2. In Supporting Information movie S1, the growth rate of the PtSi growing within a Si nanowire without oxide was about 5 nm/sec, while in movie S2, that of the PtSi growing within a Si nanowire with 2 nm-thick oxide was about 0.05 nm/sec. The rate difference by two orders of magnitude resulted from oxide acting as a diffusion barrier. Notably, continuous growth was seen in Supporting Information movie S1; however, it was stepwise growth that was observed in movie S2, where an incubation time was needed for nucleation and growth with a limited number of Pt atoms supporting the silicide formation. This is coherent with our previous studies.[40]

In order to understand the role of surface oxide on the Si nanowire during the diffusion process of Pt atoms, the molecular dynamics (MD) simulations were performed based on Vienna ab-initio simulation package (VASP).[41,42] The supercell was constructed with the existence of amorphous oxide, as shown in Figure 5a.[43] The thickness of the oxide layer was varied from 0 to 1 nm. Without oxide, the Pt atoms dissolve rapidly into the Si and build up a high-concentration profile below the Pt pads; thereby, we expect the nucleation of PtSi to occur below the contact area. With oxide, the effect of the oxide behaves like a weak diffusion barrier. The Pt atoms were found to diffuse through the oxide and distribute within the Si nanowire. The distribution length actually increases as the square root of time, and the concentration profile looks like a Gaussian function. In Figure 5b, the first concentration profile depicts that when we add the two concentration profiles together, the green one from the left and the purple one from right, it indicates that an uphill diffusion of Pt has to occur. Based on the theory of nucleation and growth,[44] the diffusion of both sides should stop at the middle when they meet, because beyond that the diffusion will be against the concentration gradient of the opposite side. Thus, a build-up of concentration occurs, and it will lead to a flat concentration profile in the middle. The interdiffusion will lead to saturation of Pt in the Si

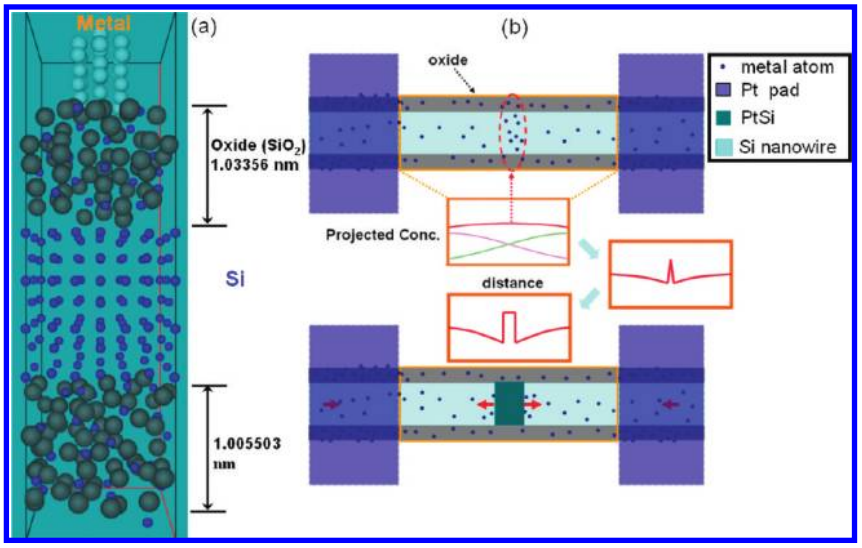

Figure 5. Simulation of oxide effect in kinetics of nanosilicide formation. (a) Supercell consisting of Si crystal covered with amorphous SiO_2. The metal cluster situating on the top of oxide. (b) Top-view schematic plot and profiles of silicide formation with the insets of projected concentration distribution.

nanowire, which will not be an equilibrium state since the system wants to form a silicide phase, and then nucleation of a silicide can occur at any place between the two contacts due to composition fluctuation; however, the most probable place will be the middle. While the build-up might lead to a small back-flow, it is negligible. When the build-up reaches the supersaturation needed, the nucleation of PtSi occurs. After that, the change, as depicted by the third concentration profile, is similar to that of a one-dimensional precipitation. The plateau in the middle is PtSi, and the concentration at the Si/PtSi interface is an equilibrium concentration.

In summary, we have demonstrated that with or without surface oxide on the Si nanowire, different PtSi/Si nanowire heterostructures appear due to different growth mechanisms by using in situ TEM observations. Specifically, when a Si nanowire has no oxide, PtSi formation starts at the contact area between the Si nanowire and the Pt pads so that a nanoheterostructure of PtSi/Si/PtSi appears. When a Si nanowire has oxide, PtSi formation starts near the center of the Si nanowire between the two Pt pads or from one end of a Si nanowire, leading to the formation of Si/PtSi/Si nanowire-heterostructures. Additionally, it has been observed that the existence of oxide seriously affects not only the growth position but also the growth behavior and rate. Molecular dynamics simulation results are coherent with our experimental observations and the proposed growth mechanisms. Since one-dimensional nanoheterostructures may have potential applications in nanoelectronic devices, the fundamentals of nanoheterostructure growth are of great importance for future device fabrication.

■ ASSOCIATED CONTENT

Supporting Information. Two in situ TEM videos as supplementary online material to present dynamic observation of the PtSi/Si/PtSi nanoheterostructure formation and illustrate our study of oxide effects and the growth kinetics. This material is available free of charge via the Internet at http://pubs.acs.org.

■ AUTHOR INFORMATION

Corresponding Author

*E-mail: gkclu@mail.ncku.edu.tw; wwwu@mail.nctu.edu.tw; ljchen@mx.nthu.edu.tw.

Author Contributions

‖These authors contributed equally.

■ ACKNOWLEDGMENT

K.C.L., W.W.W. and L.J.C. acknowledge the support by National Science Council through grant 98-2218-E-006-249, 99-2221-E-006-131, 97-2218-E-009-027-MY3, 99-2120-M-007-011, and 98-2221-E-007-104-MY3. K.N.T., acknowledges the support of NSF/NIRT project CMS-0506841. We are also grateful to the National Center for High-Performance Computing for computer time and facilities.

■ REFERENCES

(1) Duan, X.; Huang, Y.; Cui, Y.; Wang, J.; Lieber, C. M. *Nature* **2000**, *409*, 66–69.
(2) Cui, Y.; Lieber, C. M. *Science* **2001**, *291*, 851–853.
(3) Huang, Y.; Duan, X.; Cui, Y.; Lauhon, L. J.; Kim, K.; Lieber, C. M. *Science* **2001**, *294*, 1313–1317.
(4) Xia, Y.; Yang, P.; Sun, Y.; Wu, Y.; Mayers, B.; Gates, B.; Yin, Y.; Kim, F.; Yan, H. *Adv. Mater.* **2003**, *15*, 353–389.
(5) Huang, Y.; Duan, X.; Cui, Y.; Lieber, C. M. *Nano Lett.* **2002**, *2*, 101–104.
(6) Cui, Y.; Duan, X.; Hu, J.; Lieber, C. M. *J. Phys. Chem. B* **2000**, *104*, 5213–5216.
(7) Zheng, G.; Lu, W.; Jin, S.; Lieber, C. M. *Adv. Mater.* **2004**, *16*, 1890–1893.
(8) Zhong, Z.; Wang, D.; Cui, Y.; Bockrath, M. W.; Lieber, C. M. *Science* **2003**, *302*, 1377–1379.
(9) Duan, X.; Niu, C.; Sahi, V.; Chen, J.; Parce, J. W.; Empedocles, S.; Goldman, J. *Nature* **2003**, *425*, 274–278.
(10) Duan, X. *MRS Bull.* **2007**, *32*, 134–141.
(11) Javey, A.; Nam, S.; Friedman, R. S.; Yan, H.; Lieber, C. M. *Nano Lett.* **2007**, *7*, 773–777.
(12) Patolsky, F.; Zheng, G.; Hayden, O.; Lakadamyali, M.; Zhuang, X.; Lieber, C. M. *Proc. Natl. Acad. Sci. U.S.A.* **2004**, *101*, 14017–14022.

(13) Patolsky, F.; Timko, B. P.; Zheng, G.; Lieber, C. M. *MRS Bull.* **2007**, *32*, 142–149.
(14) Schmitt, A. L.; Bierman, M. J.; Schmeisser, D.; Himpsel, F. J.; Jin, S. *Nano Lett.* **2006**, *6*, 1617–1621.
(15) Schmitt, A. L.; Zhu, L; Schmeisser, D.; Himpsel, F. J.; Jin, S. *J. Phys. Chem. B* **2006**, *110*, 18142–18146.
(16) Song, Y.; Schmitt, A. L.; Jin, S. *Nano Lett.* **2007**, *7*, 965–969.
(17) Wu, Y.; Xiang, J.; Yang, C.; Lu, W.; Lieber, C. M. *Nature* **2004**, *430*, 61–65.
(18) Lu, K. C.; Tu, K. N.; Wu, W. W.; Chen, L. J.; Yoo, B. Y.; Myung, N. V. *Appl. Phys. Lett.* **2007**, *90*, 253111.
(19) Lu, K. C.; Wu, W. W.; Wu, H. W.; Tanner, C. M.; Chang, J. P.; Chen, L. J.; Tu, K. N. *Nano Lett.* **2007**, *7*, 2389–2394.
(20) Weber, W. M.; Geelhaar, L.; Graham, A. P.; Unger, E.; Duesberg, G. S.; Liebau, M.; Pamler, W.; Cheze, C.; Riechert, H.; Lugli, P.; Kreupl, F. *Nano Lett.* **2006**, *6*, 2660–2666.
(21) Lin, Y. C.; Lu, K. C.; Wu, W. W.; Bai, J. W.; Chen, L. J.; Tu, K. N.; Huang, Y. *Nano Lett.* **2008**, *8*, 913–918.
(22) Bucher, E.; Schulz, S.; Lux-Steiner, M. C.; Munz, P.; Gubler, U.; Greuter, F. *Appl. Phys. A: Mater. Sci. Process* **1986**, *40*, 71–77.
(23) Hsu, H. C.; Wu, W. W.; Hsu, H. F.; Chen, L. J. *Nano Lett.* **2007**, *7*, 885–889.
(24) Wang, Z. L.; Ponchara, P.; de Heer, W. A. *Pure Appl. Chem.* **2000**, *72*, 209–219.
(25) Ross, F. M. *IBM J. Res. Dev.* **2000**, *44*, 489–501.
(26) Stach, E. A.; Pauzauskie, P. J.; Kuykendall, T.; Goldberger, J.; He, R.; Yang, P. *Nano Lett.* **2003**, *3*, 867–869.
(27) Golberg, D.; Li, Y. B.; Mitome, M.; Bando, Y. *Chem. Phys. Lett.* **2005**, *409*, 75–80.
(28) Law, M.; Zhang, X. F.; Yu, R.; Kuykendall, T.; Yang, P. *Small* **2005**, *1*, 858–865.
(29) Liao, C. N.; Chen, K. C.; Wu, W. W.; Chen, L. J. *Appl. Phys. Lett.* **2005**, *87*, 141903.
(30) He, J. H.; Wu, W. W.; Chueh, Y. L.; Hsin, C. L.; Chen, L. J.; Chou, L. J. *Appl. Phys. Lett.* **2005**, *87*, 223102.
(31) Liu, C. H.; Wu, W. W.; Chen, L. J. *Appl. Phys. Lett.* **2006**, *88*, 023117.
(32) Liu, C. H.; Wu, W. W.; Chen, L. J. *Appl. Phys. Lett.* **2006**, *88*, 133112.
(33) Lang, C.; Kodambaka, S.; Ross, F. M.; Cockayne, D. J. H. *Phys. Rev. Lett.* **2006**, *97*, 226104.
(34) Chen, K. C.; Wu, W. W.; Liao, C. N.; Chen, L. J.; Tu, K. N. *Science* **2008**, *321*, 1066–1069.
(35) Hannon, J. B.; Kodambaka, S.; Ross, F. M.; Tromp, R. M. *Nature* **2006**, *440*, 69.
(36) Cui, Y.; Lauhon, L. J.; Gudiksen, M. S.; Wang, J.; Lieber, C. M. *Appl. Phys. Lett.* **2001**, *78*, 2214–2216.
(37) Wagner, R. S.; Ellis, W. C. *Appl. Phys. Lett.* **1964**, *4*, 89–90.
(38) Lin, Y. C.; Chen, Y.; Xu, D.; Huang, Y. *Nano Lett.* **2010**, *10*, 4721–4726.
(39) Wu, W. W.; Lu, K. C.; Wang, C. W.; Hsieh, H. Y.; Chen, S. Y.; Chou, Y. C.; Yu, S. Y.; Chen, L. J.; Tu, K. N. *Nano Lett.* **2010**, *10*, 3984–3989.
(40) Chou, Y. C.; Lu, K. C.; Tu, K. N. *Mater. Sci. Eng., R* **2010**, *70*, 112–125.
(41) Kresse, G.; Hafner, J. *Phys. Rev. B* **1993**, *47*, 558–561.
(42) Kresse, G.; Furthmüller, J. *Phys. Rev. B* **1996**, *54*, 11169–11186.
(43) Ouyang, H.; Chiou, H. H.; Wu, Y. C. S.; Cheng, J. H.; Ouyang, W. *J. Appl. Phys.* **2007**, *102*, 013710.
(44) Porter, D. A.; Easterling, K. E. *Phase Transformations in Metals and Alloys*, 2nd ed.; Nelson Thornes Publishing: Cheltenham, U.K., 1992.